



# Hysteresis of phytoplankton communities over Sub-polar North Atlantic to CO2 forcing 2

3

Dong-Geon Lee<sup>1</sup>, Eun Young Kwon<sup>3</sup>, Jonghun Kam<sup>1</sup>, Jong-Seong Kug<sup>2\*</sup> 4

5 <sup>1</sup>Division of Environmental Science and Engineering, Pohang University of Science and Technology (POSTECH),

Pohang, South Korea

- 7 <sup>2</sup>School of Earth and Environmental Sciences, Seoul National University, Seoul, South Korea 8
  - <sup>3</sup>IBS Center for Climate Physics, Pusan National University, Busan, South Korea

9 10

Correspondence to: Jong-Seong Kug (jskug@snu.ac.kr)

11 12

13

14

15

16

17

18

19

20

21

Abstract. Marine phytoplankton play a crucial role in the ocean's food web, marine ecosystems, and the carbon cycles. Their responses to external forcing vary across phytoplankton species, and phytoplankton community shifts can have important implications for their roles in the Earth's system. Here, we find that phytoplankton communities in the Sub-Polar North Atlantic shift towards smaller species under greenhouse warming that is not easily recovered even under CO<sub>2</sub> removal scenarios. Despite negative CO<sub>2</sub> emissions, the persistent collapse of larger-celled diatom populations and shift toward smaller phytoplankton communities is a consequence of lower surface nutrient availability followed by the slowdown of the Atlantic Meridional Overturning Circulation (AMOC). This weakening of AMOC and associated nutrient transport exhibit delayed recovery. Depleting nutrients disrupt trophic dynamics, by altering primary limiting nutrient components, contributing to the continued decrease in diatoms and increase in smaller phytoplankton. Consequently, the downsizing of the phytoplankton

22 community indicates a large reduction in the ocean's biological carbon export capacity.





### Introduction

The increase in anthropogenic carbon dioxide (CO<sub>2</sub>) emissions is warming our planet. This poses a threat to nature, human beings, terrestrial and marine ecosystems, and climate systems, making global transnational efforts crucial to reduce additional carbon emissions (Gattuso et al., 2015; Cui et al., 2024; Nagelkerken and Connell, 2015). To do this, world leaders pledged in the 2015 Paris Agreement to limit longterm temperature increases to below 2°C, or ideally 1.5°C. Therefore, climate mitigation strategies, including negative CO<sub>2</sub> emissions through the development of Carbon Dioxide Removal (CDR) techniques are necessary to curb global warming (Van Vuuren et al., 2018; Meinshausen et al., 2009; Rogelj et al., 2016; Gasser et al., 2015; Tong et al., 2019). However, the Earth's climate system may not be fully recovered, even if external forcing returns to baseline conditions, known as climate irreversibility. Numerous studies have reported that several physical variables have irreversible changes on a global & regional scale including temperature, precipitation, and ocean circulation under negative CO2 emissions (Liu et al., 2023; Kim et al., 2022; Kug et al., 2022; Pathirana et al., 2023; An et al., 2022; Song et al., 2022; Boucher et al., 2012; Jeltsch-Thömmes et al., 2020; Hawkins et al., 2011). Irreversible changes in biological aspects have also been documented in both marine and terrestrial ecosystems, such as vegetation, wildfires, permafrost, primary productivity, and the carbon cycle (Park and Kug, 2022; John et al., 2015; Schwinger and Tjiputra, 2018). Despite the wealth of research on climate irreversibility, few studies have focused on changes in phytoplankton communities, which play a crucial role in the global carbon cycle.

Marine phytoplankton form the foundation of ocean ecosystems (Richardson and Schoeman, 2004; Platt et al., 2003), mediate biogeochemical processes, and regulate climate (Field et al., 1998; Behrenfeld et al., 2006; Passow and Carlson, 2012). They are responsible for nearly half of the global primary production (PP; Field et al., 1998; Falkowski et al., 1998; Behrenfeld et al., 2006). Phytoplankton are vulnerable to climate change due to their sensitivity to external environmental conditions such as temperature (Behrenfeld et al., 2006; Doney, 2006; Anderson et al., 2021; Archibald et al., 2022), insolation (Marinov et al., 2010), and nutrient availability (Moore et al., 2013). Responses to external forcing vary among phytoplankton species, so the compositions of the phytoplankton community can influence their roles in food web organization and biogeochemical processes. Therefore, shifts in phytoplankton communities play a key role in various aspects, comparable to changes in their biomass (Winder and Sommer, 2012; Barton et al., 2016) and have significant socio-economic implications for fisheries and higher ecosystem levels. Conversely, changes in these aspects can also impact phytoplankton communities (Platt et al., 2003; Reid et al., 2000).

Previous studies have argued for a trend towards smaller phytoplankton communities under warmer climates using model simulations and observation-based research (Doney, 2006; Morán et al., 2010; Winder and Sommer, 2012; Cael et al., 2021; Henson et al., 2021). This downsizing of phytoplankton communities is likely to persist even under negative CO<sub>2</sub> emissions due to the irreversible responses of physical factors predicted under carbon mitigation scenarios. As smaller phytoplankton species dominate over larger cell-sized phytoplankton, photosynthesis becomes less efficient, and the gravitational sinking of particulate organic carbon (POC) in the oceans weakens, reducing the amount of carbon sequestered over time (Boyd and Trull, 2007; Guidi et al., 2009;





Maranon, 2014).

The Subpolar North Atlantic (SPNA) Ocean is not only a critical region for climate change but also plays a vital role in the biological processes that govern CO<sub>2</sub> gas exchange between the air and seas (Manabe and Stouffer, 1995; Sabine et al., 2004; Bennington et al., 2009). Under global warming scenarios, there is a counterintuitive decrease in temperature in this region, resulting from the weakening of the Atlantic Meridional Overturning Circulation (AMOC), which drives deep convection in the SPNA region (Caesar et al., 2018; Liu et al., 2020; Oh et al., 2022). The weakening of the AMOC under global warming impairs volume transport from low to high latitudes, accompanied by decreases in nutrient-rich water conveyance (Schmittner, 2005). The SPNA region is one of the most significant areas for carbon uptake in the current regional climate and carbon cycle (Sabine et al., 2004). Nutrient deficiencies in the SPNA region potentially lead to shifts in plankton composition, resulting in large decreases in export production (EP) and net primary productivity (NPP) under future climate conditions. Previous studies have examined decreases in marine productivity in the SPNA under global warming (Schmittner, 2005; Steinacher et al., 2010; Moore et al., 2013). Despite the irreversibility of AMOC strength revealed by other studies, the irreversible responses of phytoplankton communities in this region have not been thoroughly explored.

Here, we aim to examine phytoplankton community shifts under negative CO<sub>2</sub> emissions and their implications as biological climate regulators. First, we analyze idealized CO<sub>2</sub> emission-driven simulations based on the Community Earth System Model 2 (CESM2) with multiple ensembles. The simulations incorporate biogeochemical processes coupled with a biogeochemistry model, and it simulate three explicit phytoplankton functional types (PFTs): diatoms, small phytoplankton, and diazotrophs (See Methods for details). In the following sections, we report irreversible shifts in phytoplankton communities in the SPNA region and examine the mechanisms driving these results.





### Methods

## Model Configuration

In this study, we employed Community Earth System Model version 2 (CESM2) to investigate marine biogeochemical cycles, focusing on the dynamics of the nutrient and phytoplankton communities in the SO. The marine ecosystem within CESM2 is represented by the Marine Biogeochemical Library (MARBL), which incorporates three explicitly modeled phytoplankton functional groups—diatoms, diazotroph, pico/nano (small) phytoplankton—as well as one implicit group (calcifiers) and single zooplankton group. MARBL also simulates 32 different tracers, which include 17 abiotic constituents such as dissolved inorganic and organic carbon, alkalinity, nutrients, and oxygen, along with 15 biotic tracers associated with phytoplankton biomass (e.g., Carbon (C), Phosphorus (P), Silica (Si), Iron (Fe), and Calcium Carbonate (CaCO<sub>3</sub>)), as well as zooplankton carbon.

Within MARBL, phytoplankton growth rates depend on multiple environmental parameters, including temperature, nutrient limitation, and light availability as detailed in Long et al. (2021). Nutrient limitation is determined by Leibig's law of the minimum, whereby the nutrient available in the smallest quantities limits phytoplankton growth. Changes in PFT concentrations are calculated by source (i.e., net primary productivity) and sink (grazing, linear mortality, and aggregation) terms as elaborated in Long et al (2021).

Long et al (2021)(Long et al., 2021) evaluated the model's performance in simulating biogeochemical variables such as macronutrient (Nitrate; NO<sub>3</sub>, Phosphate; PO<sub>4</sub>, Silicate; SiO<sub>3</sub>) distribution and NPP and export production (EP). They showed that MARBL effectively simulates the geographical patterns of macronutrients in the SPNA region compared to World Ocean Atlas (WOA) observations. Moreover, comparisons with satellite observations revealed that the global distribution of NPP simulated by MARBL exhibits similar patterns, albeit with slight differences in magnitude.

# **Experimental Design**

We analyzed an idealized negative CO<sub>2</sub> emissions pathway that effectively reduces emissions incrementally, considering the development of Carbon Dioxide Removal (CDR) technology and global mitigation efforts. In our experiments, anthropogenic CO<sub>2</sub> emissions increase linearly from an initial CO<sub>2</sub> concentration of 383 ppm to the year 2050, based on the SSP5-8.5 scenario. Subsequently, emissions decrease at the same rate until the global mean atmospheric CO<sub>2</sub> concentration returns to its original value (in the year 2196). Immediately after reaching this level, net-zero emissions are maintained until the end of the simulation (year 2400). The atmospheric CO<sub>2</sub> level peaks in the year 2107 (725 ppm), just a few years before achieving net-zero emission. For better readability, we define periods as follows: Ramp-up and -down period as CO<sub>2</sub> increasing period (2001-2107) and decreasing period (2108-2196), and restoring period as the duration of net-zero emission (2197-2400), respectively. We also have defined the first 11 years (2001-2011) as the "Climatology period", and the 11 years (2191-2201) at the end of the ramp-down as the "CO<sub>2</sub> down period" to identify hysteresis of climatic variables

https://doi.org/10.5194/egusphere-2025-1474 Preprint. Discussion started: 17 April 2025 © Author(s) 2025. CC BY 4.0 License.





- under the same CO<sub>2</sub> conditions. We have run total of nine ensemble members each with slightly different initial
- 116 conditions to consider the variability.





Results

### Irreversible phytoplankton community shifts to CO2 forcing in SPNA region

We investigate the shifts in phytoplankton communities between the climatology period and the CO<sub>2</sub> down period. The statistical method known as Bray-Curtis (BC) dissimilarity was used to examine the similarity of the phytoplankton communities between the two periods following Cael et al (2021). The BC method is frequently utilized in ecology and biology to quantify differences in species composition between two sites (Bray et al., 1957; Herren and McMahon, 2017). Therefore, in our study, we numerically determined the degree of shifts in the diversity of PFTs between the two periods under comparison. The BC method is calculated as below:

$$Bray - Curtis\ dissimilarity\ (BC) =$$

$$1 - 2\sum_{i}^{R} \min \left( B_{2000-2010}^{i}, B_{2192-2202}^{i} \right) / \sum_{i}^{R} \left( B_{2000-2010}^{i} + B_{2192-2202}^{i} \right)$$
 (1)

 $B_t^i$  represents the average biomass for PFT i over year(s) t, and R is the number of PFTs, hence it is 3 in this simulation. There are pronounced positive values (indicating less similarity) of dissimilarity at high latitudes in the northern hemisphere (NH), including the Arctic and SPNA region, as well as near the frontal zones of the Southern Ocean (SO) (Fig. S1). Notably, the most significant shifts in phytoplankton communities emerge in the SPNA region, indicating substantial variations in phytoplankton composition (Fig. 1a).

Fig. 1b presents a time series of area-averaged PFT biomass in the SPNA region. As atmospheric CO<sub>2</sub> concentrations increase, diatoms and small phytoplankton exhibit significant decrease and increase, respectively. These results are consistent with previous studies, which have reported shifts towards smaller PFT-dominant phytoplankton communities in a warmer world (Doney, 2006; Morán et al., 2010; Cael et al., 2021; Henson et al., 2021; Winder and Sommer, 2012). These variations in PFT biomass persist under negative CO<sub>2</sub> emissions. While small phytoplankton increase over time and has a peak in the middle of the ramp-down period, diatoms continue to decrease and have a minimum value at the same time. Similarly, the diazotroph concentrations decrease, except for a slight initial increase, eventually reaching a minimum at the end of the ramp-down period. During the restoring period, all PFTs—except diazotrophs, which overshoot—return to near their initial values with diatom concentrations showing a slight weakening. Comparing the two periods (CO<sub>2</sub> down - Climatology) with the same atmospheric CO<sub>2</sub> concentration reveals substantial shifts in the phytoplankton community. Specifically, there is a large decrease in larger cell-sized phytoplankton and an increase in smaller cell-sized phytoplankton, indicating significant downsizing of the phytoplankton community.

All PFTs exhibit strong hysteresis in response to CO<sub>2</sub> forcing (Figs 1c-e). In particular, diatom concentrations decreased to 24% of their initial value during the ramp-up period, while small phytoplankton increased by about 283% compared to the Climatology period. The phytoplankton biomass remained nearly





constant during the ramp-down period when the atmospheric CO<sub>2</sub> concentration returned to its initial value of 383 ppm. These results indicate shifts in the phytoplankton community towards dominance by smaller phytoplankton in the SPNA region, despite the same atmospheric CO<sub>2</sub> concentration. In addition, although the diazotroph concentrations constitute a relatively smaller portion of the total PFTs, their pronounced decline during the ramp-down period leads to a weakening of biological N fixation to the ocean (Fig. S2a). The diazotrophs show different behavior compared to the other two species because of their temperature-limited biological properties (Breitbarth et al., 2007; Yi et al., 2020). Consequently, temporal changes in Sea Surface Temperature (SST), diazotroph concentrations, and N fixation rates in the SPNA region are all closely aligned (Fig. S2).

Smaller phytoplankton have greater competitiveness in oligotrophic and stratified marine environments in a warmer world due to their enhanced surface area-to-volume ratio (Winder and Sommer, 2012; Morán et al., 2010). Within MARBL—the biogeochemical component of the CESM2 Earth System Model—the advantage of smaller phytoplankton in low-nutrient environments is parametrized via half-saturation coefficients (Long et al., 2021). For instance, two PFTs (diatom and small phytoplankton) may possess the same maximum growth rate; however, the half-saturation coefficient is parameterized to be smaller for small phytoplankton. This implies that small phytoplankton can achieve their maximum growth rate with a lower nutrient concentration. Furthermore, the decrease in diatoms due to the shift towards oligotrophic conditions may lead to a reduction in zooplankton and a weakening of grazing by higher-level predators, thereby promoting the growth of small phytoplankton. The time series of source and sink terms integrated to 100 m depth exhibits that grazing is the dominant sink contribution to loss for both PFTs, with other terms having relatively minor effects (Fig. S3).

# Hysteresis of AMOC strength and shift in primary nutrient limiting component.

The spatial distribution of PFT biomass differences between the two periods reveals a significant shift across the SPNA (Figs. 2a-c). Across the entire Atlantic and Arctic regions, and even globally (not shown), the most dramatic differences are observed in the SPNA region. For diazotrophs, whose growth rates are temperature-dependent, high latitudes above 50°N exhibit scant biomass climatologically and no variations (Fig. S4, Fig. 2c). Except for diazotrophs, changes in phytoplankton concentrations are generally driven by nutrient availability. While NO<sub>3</sub> is commonly considered the most limiting nutrient globally, observation-based studies have identified silicate as the primary limiting component for phytoplankton growth in the SPNA region (Allen et al., 2005). The CESM2 biogeochemical model, MARBL, also well simulates Si-limited growth of diatoms in the SPNA region, consistent with observations (Long et al., 2021). The spatial distribution of differences between the two periods for both macronutrients (NO<sub>3</sub>, SiO<sub>3</sub>) shows similar patterns to PFT biomass changes.

The North Atlantic, including the SPNA region, is characterized by deep convection associated with the AMOC. Changes in the AMOC lead to significant physical alterations in the SPNA region. In particular, the AMOC plays a pivotal role in transporting water volumes from low to high latitudes, and through this process, nutrient-rich water transport can trigger biological changes (Boot et al., 2023). Under global warming, AMOC is





expected to progressively weaken due to increased surface temperature and the influx of freshwater. Additionally, it has been reported that under negative emissions, AMOC strength will not recover immediately but will instead decrease further with a delay. This implies that changes in AMOC strength may influence shifts in the phytoplankton community in the SPNA region under a climate mitigation scenario.

Thus, we investigate the changes in AMOC strength and nutrient concentrations in our simulations (Fig. 3a). In our experiments, the intensity of the AMOC continues to decrease with increasing atmospheric CO<sub>2</sub> concentration, persisting until the middle of the CO<sub>2</sub> mitigation pathway and reaching its weakest state around the year 2142 (Fig. 3a). Subsequently, the AMOC gradually strengthens again, returning to its initial condition with overshooting during the restoring period (Wu et al., 2011; Jackson et al., 2014; An et al., 2021). Consistent with the weakening of AMOC strength over time, both nutrient concentrations also continue to decline (Fig. 3a). Interestingly, while both nutrients decline over time, the reduction in SiO<sub>3</sub> concentration halts around the year 2075 and remains steady until approximately the year 2250 before recovering. Conversely, NO3 decreases until around the year 2170, past the point of minimal AMOC strength, and then recovers with the AMOC turnabout. The distinct responses of SiO<sub>3</sub> and NO<sub>3</sub> to CO<sub>2</sub> forcing arise largely due to the diverging responses of PFTs from the climatology period to the CO<sub>2</sub> down period. While decreases in diatoms-driven NPP reduce the consumption rates of both SiO<sub>3</sub> and NO<sub>3</sub>, increases in small-phytoplankton-driven NPP counterbalance the decreasing NO<sub>3</sub> consumption rates, resulting in a more persistent decline in NO<sub>3</sub>. Reduced diazotrophs-driven NPP and associated N-fixation also contribute to further decline in surface NO<sub>3</sub> concentrations. Changes in the limiting nutrient components may affect the nutrient dynamics of phytoplankton, particularly diatoms, which are composed of larger cells in the SPNA region.

We identified changes in the limiting nutrients for the growth of two PFTs (diatom, small phytoplankton). The spatial patterns of limiting nutrients are shown in Fig. 3c and 3d for diatoms and in Fig. S5c and Fig. S5d for small phytoplankton, with the SPNA-averaged time series are shown in Fig. 3b and Fig. S5a. When spatially averaged, small phytoplankton, unaffected by SiO<sub>3</sub> availability experience N limitation throughout all timeframes owing to continuously decreasing NO<sub>3</sub> levels (Fig. S5). For diatoms, however, the predominant limiting nutrient shifts from Silicon (Si) to N around the year 2076, coinciding with the stabilization of SiO<sub>3</sub> levels (Figs. 3a-b). During the Climatology period, Si limitation for diatom dominates across most of the SPNA region (Fig 3c). However, as NO<sub>3</sub> decreases more rapidly than SiO<sub>3</sub>, N limitation spreads across the SNPA region, eventually overtaking Si limitation. By the CO<sub>2</sub> down period, Si limitation becomes only confined to small regions, with most areas transitioning to N limitation. (Figs. 3c-d).

From the Irminger Sea, located beneath Greenland to the Nordic Sea, the Si-limited environment persists even during the CO<sub>2</sub> down period. This region, characterized by intense deep convection in the present climate (Renssen et al., 2005; Heuzé, 2017), exhibits the most pronounced shallowing of the mixed layer depth (MLD) than elsewhere, indicating that it is particularly affected by the weakening of the AMOC (Fig. S6). Consequently, SiO<sub>3</sub> concentrations are significantly reduced compared to other regions, maintaining Si limitation. Furthermore, even as the AMOC enters a recovery phase, nutrient levels do not rebound immediately and exhibit a delayed





response. Thus, lagged nutrient retrieval causes a corresponding lagged response in phytoplankton community recovery. As the AMOC strength and nutrient transport are reinstated, nutrient concentrations increase sufficiently by around the year 2250, causing a revert to Si limitation. This suggests that while the AMOC plays a critical role in nutrient distribution and the marine ecosystem in the SPNA region, the phytoplankton community may experience stronger hysteresis than the recovery of AMOC strength under a climate mitigation scenario.

226

227

228

229

230

231

232

233

234

235

236

237

238

239

240

241

242

243

244

245

246

247

248

249

250

251

221

222

223

224

225

#### Implication of phytoplankton community shift on POC export

The shift towards smaller phytoplankton communities can have significant ecological, biogeochemical, and climatic impacts. Phytoplankton composed of larger cells, possess a greater capacity for sequestering CO<sub>2</sub> through photosynthesis and gravitational sinking into the ocean. In contrast, organic carbon exported by smaller phytoplankton is more readily degraded by higher-level predators such as bacteria and zooplankton, and can be re-released back to the water column as CO<sub>2</sub> quickly compared to diatoms (Leblanc et al., 2018; Tréguer et al., 2018). Therefore, the collapse of diatom populations during the CO<sub>2</sub> down periods could lead to a loss of biological carbon sequestration competence (biological pump). This attenuation is particularly evident in the SPNA region, where the phytoplankton community shifts are most pronounced (Fig. 4a). The weakening of the biological pump is evident throughout the SNPA region and extends beyond in parts of the Arctic region. Consistent with the strong biological hysteresis observed in the above results, there is a significant irreversible decline in the organisms' ability to export carbon (POC flux). The abundance of diatoms, which typically dominate the biological carbon pump, has decreased to about a fourth, while small phytoplankton have increased by a factor of 2.7. As a result, when CO<sub>2</sub> concentrations return to initial levels, the POC flux is less than half of the initial condition, indicating that the decrease in diatoms plays a dominant role in POC export changes. Specifically, the SPNA region, currently a key area for CO2 sequestration (Sabine et al., 2004), is projected to be less effective at exporting carbon than the global average after CO<sub>2</sub> mitigation (Figs 4b-c). Consequently, while the North Atlantic Ocean is presently known for its strong biological pump, it may lose its prestige under CO2 mitigation scenarios (Fig. 4). Therefore, the longer climate mitigation is delayed, the more the miniaturization of phytoplankton communities will accelerate, further slowing down the marine biological pump.

Therefore, even if atmospheric CO<sub>2</sub> concentrations return to their original levels through negative emissions, marine ecosystems, especially the composition of PFTs will exhibit strong hysteresis. This disrupted phytoplankton community has the potential to impact regional & global trophic dynamics and food webs, as well as commercial fisheries and more. Moreover, if global warming accelerates again in the context of a downsizing of the phytoplankton community, it is possible that we will experience even more abrupt climate change than at present, as the Earth's capacity for biological carbon export is diminished.

252253

254

# Discussion





This study conducts idealized CO<sub>2</sub> emission-driven simulations using multiple ensembles to investigate how phytoplankton communities respond under CO<sub>2</sub> mitigation scenarios. When atmospheric CO<sub>2</sub> concentration returns to initial levels through negative emissions, we observe the most significant changes in the composition of PFTs in the SPNA region (Fig. 1a). For example, smaller phytoplankton populations increase, and the concentrations of large cell-sized diatoms collapse (Figs. 1b-d). The diazotroph concentrations significantly decrease, reflecting the response to oceanic temperature changes (Fig. 1b, e, Fig. S2). Across the SPNA region, macronutrients (NO<sub>3</sub>, SiO<sub>3</sub>) can substantially limit phytoplankton growth (Figs. 2d-e, Fig. 3a). As the globe warms, the AMOC gradually weakens and exhibits strong hysteresis under negative CO2 emission. The reductions in nutrient concentrations are strongly correlated with AMOC weakening (Fig. 3a). The weakening of the AMOC leads to regional and global climatic variations, particularly affecting nutrient transport, which is essential for biological activities in the SPNA region. Furthermore, shifts in the phytoplankton community alter trophic dynamics, accelerating NO<sub>3</sub> depletion, and creating an N-limited environment for diatom growth (Fig. 3b). The downsizing of the phytoplankton community is markedly slow to recover, even as AMOC strength rebounds, due to the delayed recovery of nutrient levels. Consequently, PFTs exhibit hysteresis, which could have significant biological, biogeochemical, and climatic implications. Carbon export capacity in the SPNA region is exacerbated by more than 50% compared to the present climate.

Our study reveals that global warming-driven hysteresis in AMOC strength can trigger hysteresis not only in physical parameters, such as SST and salinity but also in cascading biological and biogeochemical responses. Pronounced shifts in phytoplankton communities in the Subpolar North Atlantic involve negative feedback, resulting in the loss of biological carbon export capacity, which in turn exacerbates global warming. In other words, multiple stressors—physical, trophic and biological—can interact and weaken the resilience of marine ecosystems and the biological carbon pump system (Conversi et al., 2015).

However, our study has several limitations and potential avenues for further research. Our study uses CO<sub>2</sub> emission-driven idealized experiments with nine ensembles but relies on a single model, CESM2, which could render the results model-dependent. It has been documented that CESM2 simulates AMOC weakening more sensitively than other Earth System Models (Schwinger et al., 2022; Needham et al., 2024), potentially leading to a propensity to overestimate marine ecosystem changes. However, the GFDL-ESM4 and CNRM-ESM2-1, as part of the CDRMIP experiments in CMIP6, include diatom variables and exhibit consistent weakening in diatom concentrations alongside AMOC weakening in the SPNA region (Fig. S8). Another limitation of this study is that the CESM2 MARBL biogeochemical model includes only three PFTs—diatoms, small phytoplankton, and diazotrophs. While this study offers valuable insights into the broader shifts in phytoplankton community structure under climate mitigation scenarios, it is essential to acknowledge the limitations of representing the complex phytoplankton community with only three PFTs. Analyzing changes in specific PFTs is beyond the scope of this study and requires further investigation of simplicity/diversity of PFTs in simulating global biogeochemical cycle. However, the model's simplicity is still advantageous in capturing future trends in phytoplankton as a function of their cell size and the underlying mechanisms driving phytoplankton dynamics and their biogeochemical

https://doi.org/10.5194/egusphere-2025-1474 Preprint. Discussion started: 17 April 2025 © Author(s) 2025. CC BY 4.0 License.



291

292

293

294

295296

297



implications. While the simplification of the CESM2 MARBL model to three PFTs could be considered a limitation, it does not diminish the significance of the results.

This study demonstrates that CESM effectively captures key trends in phytoplankton community shifts and their broader implications, providing a strong framework for assessing the impacts of climate change on marine ecosystems. This study advances our understanding of the potential trajectories of marine biogeochemical processes and their environmental and economic implications. Future research could further enhance these findings by incorporating a more diverse range of PFTs.





298 **Data Availability Statement** 299 The data used in this study will be available from https://doi.org/10.6084/m9.figshare.27058897, and the CMIP6 300 archives are freely available from https://esgf-node.llnl. gov/projects/cmip6. 301 302 Code availability 303 The computer codes that support the analysis within this paper are available from the corresponding author on 304 request. 305 306 Acknowledgements 307 This work was supported by the National Research Foundation of Korea (NRF2022R1A3B1077622). 308 309 Competing interests 310 The authors declare no competing interests. 311 312 **Author contributions** 313 DGL compiled the data, conducted analyses, prepared the figures, and wrote the manuscript. JSK designed the 314 research and wrote the majority of the manuscript content. All the authors discussed the study results and reviewed 315 the manuscript.





- 316 Reference
- 317 Allen, J. T., Brown, L., Sanders, R., Moore, C. M., Mustard, A., Fielding, S., Lucas, M., Rixen, M., Savidge, G.,
- 318 Henson, S., and Mayor, D.: Diatom carbon export enhanced by silicate upwelling in the northeast Atlantic,
- 319 Nature, 437, 728–732, https://doi.org/10.1038/nature03948, 2005.
- 320 An, S. Il, Shin, J., Yeh, S. W., Son, S. W., Kug, J. S., Min, S. K., and Kim, H. J.: Global Cooling Hiatus Driven
- by an AMOC Overshoot in a Carbon Dioxide Removal Scenario, Earth's Futur., 9,
- 322 https://doi.org/10.1029/2021EF002165, 2021.
- 323 An, S. Il, Park, H. J., Kim, S. K., Shin, J., Yeh, S. W., and Kug, J. S.: Intensity changes of Indian Ocean dipole
- mode in a carbon dioxide removal scenario, npj Clim. Atmos. Sci., 5, 1–8, https://doi.org/10.1038/s41612-022-
- 325 00246-6, 2022.
- 326 Anderson, S. I., Barton, A. D., Clayton, S., Dutkiewicz, S., and Rynearson, T. A.: Marine phytoplankton
- functional types exhibit diverse responses to thermal change, Nat. Commun., 12, 1–9,
- 328 https://doi.org/10.1038/s41467-021-26651-8, 2021.
- 329 Archibald, K. M., Dutkiewicz, S., Laufkötter, C., and Moeller, H. V.: Thermal Responses in Global Marine
- 330 Planktonic Food Webs Are Mediated by Temperature Effects on Metabolism, J. Geophys. Res. Ocean., 127, 1-
- 331 18, https://doi.org/10.1029/2022JC018932, 2022.
- 332 Barton, A. D., Irwin, A. J., Finkel, Z. V., and Stock, C. A.: Anthropogenic climate change drives shift and
- 333 shuffle in North Atlantic phytoplankton communities, Proc. Natl. Acad. Sci. U. S. A., 113, 2964–2969,
- 334 https://doi.org/10.1073/pnas.1519080113, 2016.
- 335 Behrenfeld, M. J., O'Malley, R. T., Siegel, D. A., McClain, C. R., Sarmiento, J. L., Feldman, G. C., Milligan, A.
- 336 J., Falkowski, P. G., Letelier, R. M., and Boss, E. S.: Climate-driven trends in contemporary ocean productivity,
- 337 Nature, 444, 752–755, https://doi.org/10.1038/nature05317, 2006.
- 338 Bennington, V., McKinley, G. A., Dutkiewicz, S., and Ullman, D.: What does chlorophyll variability tell us
- about export and air-sea CO 2 flux variability in the North Atlantic?, Global Biogeochem. Cycles, 23, 1-11,
- 340 https://doi.org/10.1029/2008GB003241, 2009.





- 341 Boot, A., von der Heydt, A. S., and Dijkstra, H. A.: Effect of Plankton Composition Shifts in the North Atlantic
- 342 on Atmospheric pCO2, Geophys. Res. Lett., 50, https://doi.org/10.1029/2022GL100230, 2023.
- Boucher, O., Halloran, P. R., Burke, E. J., Doutriaux-Boucher, M., Jones, C. D., Lowe, J., Ringer, M. A.,
- Robertson, E., and Wu, P.: Reversibility in an Earth System model in response to CO2 concentration changes,
- 345 Environ. Res. Lett., 7, https://doi.org/10.1088/1748-9326/7/2/024013, 2012.
- 346 Boyd, P. W. and Trull, T. W.: Understanding the export of biogenic particles in oceanic waters: Is there
- 347 consensus?, Prog. Oceanogr., 72, 276–312, https://doi.org/10.1016/j.pocean.2006.10.007, 2007.
- 348 Bray, J. R., Curtis, J. T., and Roger, J.: This content downloaded from 147.8.31.43 on Mon, Source Ecol.
- 349 Monogr., 27, 325-349, 1957.
- 350 Breitbarth, E., Oschlies, A., and LaRoche, J.: Physiological constraints on the global distribution of
- 351 Trichodesmium Effect of temperature on diazotrophy, Biogeosciences, 4, 53-61, https://doi.org/10.5194/bg-4-
- 352 53-2007, 2007.
- 353 Cael, B. B., Dutkiewicz, S., and Henson, S.: Abrupt shifts in 21st-century plankton communities, Sci. Adv., 7,
- 354 https://doi.org/10.1126/sciadv.abf8593, 2021.
- Caesar, L., Rahmstorf, S., Robinson, A., Feulner, G., and Saba, V.: Observed fingerprint of a weakening
- 356 Atlantic Ocean overturning circulation, Nature, 556, 191–196, https://doi.org/10.1038/s41586-018-0006-5,
- 357 2018.
- 358 Conversi, A., Dakos, V., Gårdmark, A., Ling, S., Folke, C., Mumby, P. J., Greene, C., Edwards, M., Blenckner,
- 359 T., Casini, M., Pershing, A., and Möllmann, C.: A Holistic view of Marine Regime shifts, Philos. Trans. R. Soc.
- 360 B Biol. Sci., 370, 1–8, https://doi.org/10.1098/rstb.2013.0279, 2015.
- 361 Cui, J., Zheng, M., Bian, Z., Pan, N., Tian, H., Zhang, X., Qiu, Z., Xu, J., and Gu, B.: Elevated CO2 levels
- promote both carbon and nitrogen cycling in global forests, Nat. Clim. Chang., 14, 511–517,
- 363 https://doi.org/10.1038/s41558-024-01973-9, 2024.
- Doney, S. C.: Plankton in a warmer world, Nature, 444, 695–696, https://doi.org/10.1038/444695a, 2006.
- 365 Falkowski, P. G., Barber, R. T., and Smetacek, V.: Biogeochemical controls and feedbacks on ocean primary





- 366 production, Science (80-.)., 281, 200–206, https://doi.org/10.1126/science.281.5374.200, 1998.
- 367 Field, C. B., Behrenfeld, M. J., Randerson, J. T., and Falkowski, P.: Primary production of the biosphere:
- 368 Integrating terrestrial and oceanic components, Science (80-.)., 281, 237–240,
- 369 https://doi.org/10.1126/science.281.5374.237, 1998.
- 370 Gasser, T., Guivarch, C., Tachiiri, K., Jones, C. D., and Ciais, P.: Negative emissions physically needed to keep
- global warming below 2°C, Nat. Commun., 6, https://doi.org/10.1038/ncomms8958, 2015.
- 372 Gattuso, J. P., Magnan, A., Billé, R., Cheung, W. W. L., Howes, E. L., Joos, F., Allemand, D., Bopp, L.,
- 373 Cooley, S. R., Eakin, C. M., Hoegh-Guldberg, O., Kelly, R. P., Pörtner, H. O., Rogers, A. D., Baxter, J. M.,
- Laffoley, D., Osborn, D., Rankovic, A., Rochette, J., Sumaila, U. R., Treyer, S., and Turley, C.: Contrasting
- futures for ocean and society from different anthropogenic CO2 emissions scenarios, Science (80-.)., 349,
- 376 https://doi.org/10.1126/science.aac4722, 2015.
- 377 Guidi, L., Stemmann, L., Jackson, G. A., Ibanez, F., Claustre, H., Legendre, L., Picheral, M., and Gorsky, G.:
- 378 Effects of phytoplankton community on production, size and export of large aggregates: A world-ocean
- analysis, Limnol. Oceanogr., 54, 1951–1963, https://doi.org/10.4319/lo.2009.54.6.1951, 2009.
- Hawkins, E., Smith, R. S., Allison, L. C., Gregory, J. M., Woollings, T. J., Pohlmann, H., and De Cuevas, B.:
- 381 Bistability of the Atlantic overturning circulation in a global climate model and links to ocean freshwater
- $382 \qquad transport, Geophys.\ Res.\ Lett., 38,\ 1-6, https://doi.org/10.1029/2011GL047208,\ 2011.$
- 383 Henson, S. A., Cael, B. B., Allen, S. R., and Dutkiewicz, S.: Future phytoplankton diversity in a changing
- 384 climate, Nat. Commun., 12, 1–8, https://doi.org/10.1038/s41467-021-25699-w, 2021.
- 385 Herren, C. M. and McMahon, K. D.: Cohesion: A method for quantifying the connectivity of microbial
- 386 communities, ISME J., 11, 2426–2438, https://doi.org/10.1038/ismej.2017.91, 2017.
- 387 Heuzé, C.: North Atlantic deep water formation and AMOC in CMIP5 models, Ocean Sci., 13, 609-622,
- 388 https://doi.org/10.5194/os-13-609-2017, 2017.
- Jackson, L. C., Schaller, N., Smith, R. S., Palmer, M. D., and Vellinga, M.: Response of the Atlantic meridional
- overturning circulation to a reversal of greenhouse gas increases, Clim. Dyn., 42, 3323–3336,





- 391 https://doi.org/10.1007/s00382-013-1842-5, 2014.
- 392 Jeltsch-Thömmes, A., Stocker, T. F., and Joos, F.: Hysteresis of the Earth system under positive and negative
- 393 CO2emissions, Environ. Res. Lett., 15, https://doi.org/10.1088/1748-9326/abc4af, 2020.
- 394 John, J. G., Stock, C. A., and Dunne, J. P.: A more productive, but different, ocean after mitigation, Geophys.
- 395 Res. Lett., 42, 9836–9845, https://doi.org/10.1002/2015GL066160, 2015.
- 396 Kim, S. K., Shin, J., An, S. Il, Kim, H. J., Im, N., Xie, S. P., Kug, J. S., and Yeh, S. W.: Widespread irreversible
- changes in surface temperature and precipitation in response to CO2 forcing, Nat. Clim. Chang., 12,
- 398 https://doi.org/10.1038/s41558-022-01452-z, 2022.
- 399 Kug, J. S., Oh, J. H., An, S. Il, Yeh, S. W., Min, S. K., Son, S. W., Kam, J., Ham, Y. G., and Shin, J.: Hysteresis
- of the intertropical convergence zone to CO2 forcing, Nat. Clim. Chang., 12, 47–53,
- 401 https://doi.org/10.1038/s41558-021-01211-6, 2022.
- Leblanc, K., Quéguiner, B., Diaz, F., Cornet, V., Michel-Rodriguez, M., Durrieu De Madron, X., Bowler, C.,
- 403 Malviya, S., Thyssen, M., Grégori, G., Rembauville, M., Grosso, O., Poulain, J., De Vargas, C., Pujo-Pay, M.,
- 404 and Conan, P.: Nanoplanktonic diatoms are globally overlooked but play a role in spring blooms and carbon
- 405 export, Nat. Commun., 9, 1–12, https://doi.org/10.1038/s41467-018-03376-9, 2018.
- 406 Liu, C., An, S. Il, Jin, F. F., Stuecker, M. F., Zhang, W., Kug, J. S., Yuan, X., Shin, J., Xue, A., Geng, X., and
- 407 Kim, S. K.: ENSO skewness hysteresis and associated changes in strong El Niño under a CO2 removal scenario,
- 408 npj Clim. Atmos. Sci., 6, https://doi.org/10.1038/s41612-023-00448-6, 2023.
- 409 Liu, W., Fedorov, A. V., Xie, S. P., and Hu, S.: Climate impacts of a weakened Atlantic meridional overturning
- 410 circulation in a warming climate, Sci. Adv., 6, 1–8, https://doi.org/10.1126/sciadv.aaz4876, 2020.
- 411 Long, M. C., Moore, J. K., Lindsay, K., Levy, M., Doney, S. C., Luo, J. Y., Krumhardt, K. M., Letscher, R. T.,
- 412 Grover, M., and Sylvester, Z. T.: Simulations With the Marine Biogeochemistry Library (MARBL), J. Adv.
- 413 Model. Earth Syst., 13, https://doi.org/10.1029/2021MS002647, 2021.
- 414 Manabe, S. and Stouffer, R. B.: Freshwater input to the North Atlantic Ocean, Nature, 378, 165–167, 1995.
- 415 Maranon, E.: Cell Size as a Key Determinant of Phytoplankton Metabolism and Community Structure, Ann.





- 416 Rev. Mar. Sci., 7, 241–264, https://doi.org/10.1146/annurev-marine-010814-015955, 2014.
- 417 Marinov, I., Doney, S. C., and Lima, I. D.: Response of ocean phytoplankton community structure to climate
- 418 change over the 21st century: Partitioning the effects of nutrients, temperature and light, Biogeosciences, 7,
- 419 3941–3959, https://doi.org/10.5194/bg-7-3941-2010, 2010.
- 420 Meinshausen, M., Meinshausen, N., Hare, W., Raper, S. C. B., Frieler, K., Knutti, R., Frame, D. J., and Allen,
- 421 M. R.: Greenhouse-gas emission targets for limiting global warming to 2°C, Nature, 458, 1158–1162,
- 422 https://doi.org/10.1038/nature08017, 2009.
- 423 Moore, C. M., Mills, M. M., Arrigo, K. R., Berman-Frank, I., Bopp, L., Boyd, P. W., Galbraith, E. D., Geider,
- 424 R. J., Guieu, C., Jaccard, S. L., Jickells, T. D., La Roche, J., Lenton, T. M., Mahowald, N. M., Marañón, E.,
- 425 Marinov, I., Moore, J. K., Nakatsuka, T., Oschlies, A., Saito, M. A., Thingstad, T. F., Tsuda, A., and Ulloa, O.:
- 426 Processes and patterns of oceanic nutrient limitation, Nat. Geosci., 6, 701–710,
- 427 https://doi.org/10.1038/ngeo1765, 2013.
- 428 Morán, X. A. G., López-Urrutia, Á., Calvo-Díaz, A., and LI, W. K. W.: Increasing importance of small
- phytoplankton in a warmer ocean, Glob. Chang. Biol., 16, 1137–1144, https://doi.org/10.1111/j.1365-
- 430 2486.2009.01960.x, 2010.
- 431 Nagelkerken, I. and Connell, S. D.: Global alteration of ocean ecosystem functioning due to increasing human
- 432 CO2 emissions, Proc. Natl. Acad. Sci. U. S. A., 112, 13272–13277, https://doi.org/10.1073/pnas.1510856112,
- 433 2015.
- 434 Needham, M. R., Falter, D. D., and Randall, D. A.: Changes in External Forcings Drive Divergent AMOC
- 435 Responses Across CESM Generations, Geophys. Res. Lett., 51, https://doi.org/10.1029/2023GL106410, 2024.
- 436 Oh, J. H., An, S. Il, Shin, J., and Kug, J. S.: Centennial Memory of the Arctic Ocean for Future Arctic Climate
- 437 Recovery in Response to a Carbon Dioxide Removal, Earth's Futur., 10, https://doi.org/10.1029/2022EF002804,
- 438 2022.
- 439 Park, S. W. and Kug, J. S.: A decline in atmospheric CO2 levels under negative emissions may enhance carbon
- retention in the terrestrial biosphere, Commun. Earth Environ., 3, 2–9, https://doi.org/10.1038/s43247-022-
- 441 00621-4, 2022.





- 442 Passow, U. and Carlson, C. A.: The biological pump in a high CO2 world, Mar. Ecol. Prog. Ser., 470, 249-271,
- 443 https://doi.org/10.3354/meps09985, 2012.
- 444 Pathirana, G., Oh, J. H., Cai, W., An, S. Il, Min, S. K., Jo, S. Y., Shin, J., and Kug, J. S.: Increase in convective
- 445 extreme El Niño events in a CO2 removal scenario, Sci. Adv., 9, 1–10, https://doi.org/10.1126/sciadv.adh2412,
- 446 2023.
- 447 Platt, T., Fuentes-Yaco, C., and Frank, K. T.: Spring algal bloom and larval fish survival off Nova Scotia,
- 448 Nature, 423, 398-399, 2003.
- 449 Reid, P. C., Battle, E. J. V., Batten, S. D., and Brander, K. M.: Impacts of fisheries on plankton community
- 450 structure, ICES J. Mar. Sci., 57, 495–502, https://doi.org/10.1006/jmsc.2000.0740, 2000.
- 451 Renssen, H., Goosse, H., and Fichefet, T.: Contrasting trends in North Atlantic deep-water formation in the
- Labrador Sea and Nordic Seas during the Holocene, Geophys. Res. Lett., 32, 1-4,
- 453 https://doi.org/10.1029/2005GL022462, 2005.
- 454 Richardson, A. J. and Schoeman, D. S.: Climate impact on plankton ecosystems in the Northeast Atlantic,
- 455 Science (80-. )., 305, 1609–1612, https://doi.org/10.1126/science.1100958, 2004.
- 456 Rogelj, J., Den Elzen, M., Höhne, N., Fransen, T., Fekete, H., Winkler, H., Schaeffer, R., Sha, F., Riahi, K., and
- 457 Meinshausen, M.: Paris Agreement climate proposals need a boost to keep warming well below 2 °c, Nature,
- 458 534, 631–639, https://doi.org/10.1038/nature18307, 2016.
- 459 Sabine, C. L., Feely, R. A., Gruber, N., Key, R. M., Lee, K., Bullister, J. L., Wanninkhof, R., Wong, C. S., R
- 460 Wallace, D. W., Tilbrook, B., Millero, F. J., Peng, T.-H., Kozyr, A., and Ono, T.: The Oceanic Sink for
- Anthropogenic CO 2 Author(s), Rios Source Sci. New Ser., 305, 367–371, 2004.
- 462 Schmittner, A.: Decline of the marine ecosystem caused by a reduction in the Atlantic overturning circulation,
- 463 Nature, 434, 628–633, https://doi.org/10.1038/nature03476, 2005.
- 464 Schwinger, J. and Tjiputra, J.: Ocean Carbon Cycle Feedbacks Under Negative Emissions, Geophys. Res. Lett.,
- 465 45, 5062–5070, https://doi.org/10.1029/2018GL077790, 2018.
- 466 Schwinger, J., Asaadi, A., Goris, N., and Lee, H.: Possibility for strong northern hemisphere high-latitude





- 467 cooling under negative emissions, Nat. Commun., 13, https://doi.org/10.1038/s41467-022-28573-5, 2022.
- 468 Song, S. Y., Yeh, S. W., An, S. Il, Kug, J. S., Min, S. K., Son, S. W., and Shin, J.: Asymmetrical response of
- 469 summer rainfall in East Asia to CO2 forcing, Sci. Bull., 67, 213–222, https://doi.org/10.1016/j.scib.2021.08.013,
- 470 2022.
- 471 Steinacher, M., Joos, F., Frölicher, T. L., Bopp, L., Cadule, P., Cocco, V., Doney, S. C., Gehlen, M., Lindsay,
- 472 K., Moore, J. K., Schneider, B., and Segschneider, J.: Projected 21st century decrease in marine productivity: A
- 473 multi-model analysis, Biogeosciences, 7, 979–1005, https://doi.org/10.5194/bg-7-979-2010, 2010.
- 474 Tong, D., Zhang, Q., Zheng, Y., Caldeira, K., Shearer, C., Hong, C., Qin, Y., and Davis, S. J.: Committed
- 475 emissions from existing energy infrastructure jeopardize 1.5 °C climate target, Nature, 572, 373–377,
- 476 https://doi.org/10.1038/s41586-019-1364-3, 2019.
- 477 Tréguer, P., Bowler, C., Moriceau, B., Dutkiewicz, S., Gehlen, M., Aumont, O., Bittner, L., Dugdale, R., Finkel,
- 478 Z., Iudicone, D., Jahn, O., Guidi, L., Lasbleiz, M., Leblanc, K., Levy, M., and Pondaven, P.: Influence of diatom
- diversity on the ocean biological carbon pump, Nat. Geosci., 11, 27–37, https://doi.org/10.1038/s41561-017-
- 480 0028-x, 2018.
- 481 Van Vuuren, D. P., Stehfest, E., Gernaat, D. E. H. J., Van Den Berg, M., Bijl, D. L., De Boer, H. S., Daioglou,
- 482 V., Doelman, J. C., Edelenbosch, O. Y., Harmsen, M., Hof, A. F., and Van Sluisveld, M. A. E.: Alternative
- pathways to the 1.5 °c target reduce the need for negative emission technologies, Nat. Clim. Chang., 8, 391-
- 484 397, https://doi.org/10.1038/s41558-018-0119-8, 2018.
- Winder, M. and Sommer, U.: Phytoplankton response to a changing climate, https://doi.org/10.1007/s10750-
- 486 012-1149-2, 1 November 2012.
- 487 Wu, P., Jackson, L., Pardaens, A., and Schaller, N.: Extended warming of the northern high latitudes due to an
- overshoot of the Atlantic meridional overturning circulation, Geophys. Res. Lett., 38, 1–5,
- 489 https://doi.org/10.1029/2011GL049998, 2011.
- 490 Yi, X., Fu, F. X., Hutchins, D. A., and Gao, K.: Light availability modulates the effects of warming in a marine
- 491 N2 fixer, Biogeosciences, 17, 1169–1180, https://doi.org/10.5194/bg-17-1169-2020, 2020.



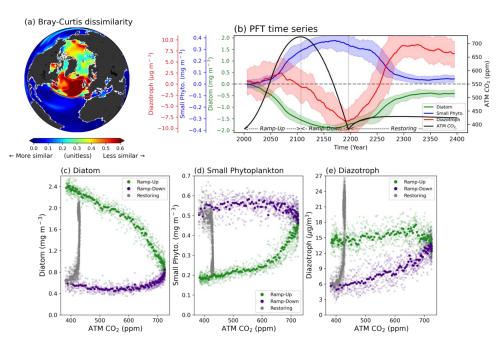


**Figure 1. (a)** Bray-Curtis dissimilarity of phytoplankton community between climatology period and CO<sub>2</sub> down period. Larger values indicate a significant change in phytoplankton composition between the two periods. **(b)** Time series of three phytoplankton functional types (PFTs). The colors in each plot represent atmospheric CO<sub>2</sub> concentration (black), diatom (green), small phytoplankton (blue), and diazotroph (red), respectively. All plots are drawn in 11-year moving averages. Shading indicates the range of minimum-maximum values between 9 ensembles. **(c-e)** Hysteresis of SPNA area-averaged biomass change (y-axis) by PFTs corresponding to global mean atmospheric CO<sub>2</sub> concentration (x-axis) for diatoms (Fig. 1c), small phytoplankton (Fig. 1d), and diazotrophs (Fig. 1e). The colors in scatters indicate the 3 periods (Ramp-up; green, Ramp-down; purple, Restoring; gray).



505

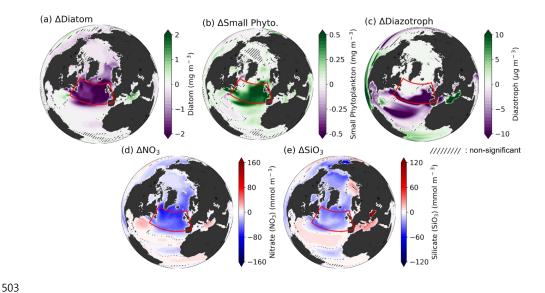


**Figure 2. (a-c)** Differences in each PFT between CO<sub>2</sub> down and climatology periods (**d-e**) Differences in macronutrients (NO<sub>3</sub>, PO<sub>4</sub>) between CO<sub>2</sub> down and climatology periods. Hatches indicate the non-significant region between 9 ensembles based on the bootstrap method.



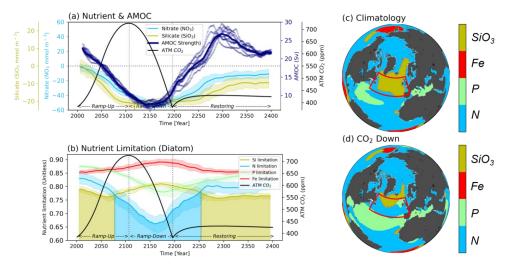


**Figure 3. (a)** Time series of strength of Atlantic Meridional Overturning Circulation (AMOC; gray), Nitrate (NO<sub>3</sub>; sky-blue), Silicate (SiO<sub>3</sub>; dark-khaki) and atmospheric CO<sub>2</sub> concentration (black) **(b)** Nutrient limitation of diatom for four nutrients (SiO<sub>3</sub>; dark-khaki, Nitrogen (N); sky-blue, Phosphorus (P); light-green, Iron (Fe); red). All plots are drawn in 11-year moving averages and the shading indicates the primary limiting nutrients for diatom growth. **(c-d)** Nutrient limitation distribution of diatom during both Climatology and CO<sub>2</sub> down period.



515

516

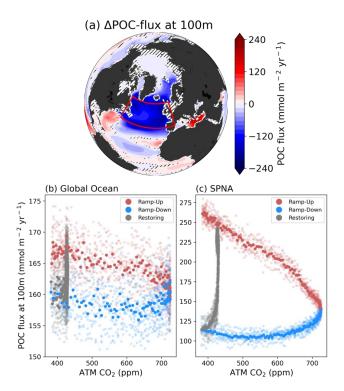


**Figure 4. (a)** Differences of Particulate Organic Carbon (POC)-flux at 100m depth between CO<sub>2</sub> down and climatology periods. **(b-c)** Hysteresis of global ocean (Fig. 4b) POC-flux at 100m depth and SPNA (Fig. 4c) region's POC-flux at 100m depth. Red color scatters indicate the Ramp-up period, blue scatters indicate the Ramp-down period and gray scatters indicate the restoring period.